NBSIR 87-3561

Thermochemistry of Materials by Laser Vaporization Mass Spectrometry, Part II - Graphite

John W. Hastie, David W. Bonnell and Peter K. Schenck

U.S. DEPARTMENT OF COMMERCE
National Bureau of Standards
Institute for Materials Science and Engineering
High Temperature Chemistry
Ceramics Division
Gaithersburg, MD 20899

June 1987

Final Report

U.S. DEPARTMENT OF COMMERCE
NATIONAL BUREAU OF STANDARDS

NBSIR 87-3561

THERMOCHEMISTRY OF MATERIALS BY LASER VAPORIZATION MASS SPECTROMETRY, PART II - GRAPHITE

John W. Hastie, David W. Bonnell and Peter K. Schenck

U.S. DEPARTMENT OF COMMERCE
National Bureau of Standards
Institute for Materials Science and Engineering
High Temperature Chemistry
Ceramics Division
Gaithersburg, MD 20899

June 1987

Final Report

U.S. DEPARTMENT OF COMMERCE, Malcolm Baldrige, *Secretary*
NATIONAL BUREAU OF STANDARDS, Ernest Ambler, *Director*

THERMOCHEMISTRY OF MATERIALS BY LASER VAPORIZATION MASS SPECTROMETRY, PART II GRAPHITE

John W. Hastie, David W. Bonnell and Peter K. Schenck
Ceramics Division
Institute for Materials Science and Engineering
National Bureau of Standards
Gaithersburg, MD 20899

Presented at the IUPAC Fifth International Conference on High Temperature and Energy-Related Materials, Rome, Italy, 25-29 May 1987.

Abstract. In an earlier study (Part I of this series) an experimental approach, which couples laser heating of refractory materials under vacuum with mass spectrometric detection of the vapor plume species for thermochemical determinations, was demonstrated using the BN refractory system at 2900 K. This paper describes the results of a similar study on polycrystalline graphite at temperatures around 4100 K and total species pressures in the vicinity of an atmosphere (1 atm = 1.01325×10^5 Nm^{-2}). A Nd/YAG laser system, focused to power densities in the region of 10^9 W/cm^2, was found to be a convenient energy source for producing thermally controlled vapor plumes and with negligible post-vaporization perturbation of the neutral species identity and concentration. The principal vapor species were found to be C_n (n = 1 - 9) and their relative intensities were found to be more consistent with the JANAF Thermochemical Tables than with other literature assessments and results. No reliable means were available to directly determine surface temperatures under the experimental conditions of very short heating times (7 - 20 ns) and luminous vapor plumes. Therefore, various indirect methods were used, including comparison of the total and partial pressure data with literature results and time-of-flight analysis of the

plume species. Surface temperatures were found to be in the range of 3800 - 4100 ± 200 K, depending on laser fluence, and the sum of the corresponding C_n species partial pressures was determined to be approximately in the range of 0.1 - 1 atm.

1 Introduction

In the preparation and application of high temperature and energy-related materials, much higher temperatures and more reactive conditions are being encountered. New or improved measurement methods are required to establish the basic thermochemical properties of materials under these aggressive conditions. For this purpose, we have developed a Laser-Induced Vaporization Mass Spectrometer system (LIVMS) which, in principle, allows for containerless measurement of species partial pressures over a wide range of temperature and pressure (Hastie et al 1984). In an earlier study on boron nitride [Part I of this series (Hastie et al 1987)], comparison of LIVMS data with JANAF (1971)-based partial pressures for B, B_2, B_3, BN, and N_2, at a surface temperature of 2900 K, indicated the presence of local thermodynamic equilibrium even for 7 ns laser pulse times. In the present study, the LIVMS technique has been further developed and applied to the graphite system.

One of the goals of this ongoing study is to develop a molecular-level understanding of the vaporization and related ionization and aggregation processes which occur when high-power laser energy is dissipated in carbon-containing materials. These highly complex processes can be expected to include the thermodynamically controlled production of C_n (n = 1 - 9) molecular species, and the non-equilibrium production of cluster species (typically, n = 10 - 1000), in addition to the formation of electrons, and

positive and negative ions. Inorganic carbon-based materials, such as graphite, metal carbides, and carbon-carbon composites, have intrinsically high resistance to thermal degradation. This behavior results from the combined effects of an inherently high sublimation energy, high melting point, and high thermal conductivity. The development of effective laser-resistant materials and obscurants is expected to rely mainly upon such carbon-based materials (Stickley 1985).

Despite considerable research over the past several decades, the basic thermodynamic, kinetic, and mechanistic description of the thermal decomposition of graphite, and related materials, is still in considerable doubt. In fact, at least three widely used but discrepant sets of thermodynamic tables exist for the carbon vapor species, the JANAF (1971, 1985) Thermochemical Tables, the so-called Livermore Tables (Leider et al 1973), and the Russian Tables (Gurvich, et al 1979). Even the melting point of graphite is a subject of considerable controversy (3800 - 5100 K range). Since the initial JANAF tabulation (1971), an appreciable number of new studies have been carried out on the graphite vaporization system. Experiments have been conducted on the effect of moderate power CO_2 and Nd-YAG lasers on the vaporization of various forms of graphite (Baker et al 1983, Covington et al 1977, Lincoln and Covington 1975, Lundell and Dickey 1977, Lundell 1982, Meyer et al 1973, Milne et al 1972, Zavitsanos 1968). Most of these studies, however, have concentrated on the macroscopic, non-molecular processes such as crater formation, material removal rate, plume dynamics, and phase equilibria.

We have reviewed the recent literature and find that there is considerable disparity among various workers, particularly concerning relative and absolute partial pressures of the various carbon polymer species (Hastie et al 1984). Analysis of the results of these literature studies indicates that the equilibrium distribution of various carbon species is still uncertain, and particularly at temperatures greater than 2800 K. Despite recent suggestions to the contrary, the JANAF (1971, 1985) tables still appear to be the most consistent with the available data. However, one cannot eliminate from consideration the possibility that this apparent data-consistency may result from offsetting errors. This could be the case, for instance, with the C_3 species which exhibits unusual entropy and vaporization coefficient characteristics. Also, the JANAF (1971, 1985) evaluation relies heavily on the Knudsen effusion mass spectrometric data of Drowart et al (1959) which were obtained at relatively low temperatures of 2700 K, and less. These workers used an ionizing electron energy of 17 eV which should reduce substantially any fragmentation effects present. However, this energy is still 2 or 3 eV above threshold for possible fragmentation pathways and recent photoionization studies of C_n (n = 3 - 20) cluster species indicate significant fragmentation of the parent positive ions near threshold energies (Geusic et al 1986). Likewise, electron impact fragmentation of S_n (n = 1 - 8) cluster species was found to be significant near threshold (Arnold et al 1986). Because of spectroscopic data uncertainties, JANAF (1971, 1985) heavily weighted the Second Law data of Drowart et al (1959), the reliability of which depends on the absence of systematic temperature error, and also on negligible electron impact fragmentation and temperature dependence affects in the ionization process.

Application of the LIVMS technique clearly provides a means to test the above concerns and the reliability of entrapolating the JANAF (1971, 1985) thermodynamic functions well beyond the experimental data limit of 2700 K imposed by the conventional Knudsen effusion mass spectrometric technique. Higher temperature access also increases the prospect of detecting the higher molecular weight C_n ($n > 5$) species predicted to be significant by the Livermore Thermochemical data analysis (Leider et al 1973). Likewise, the influence of non-unity vaporization coefficients known to be significant in the 2200 - 2700 K temperature range (eg, see Hoch et al 1974), should be greatly reduced or eliminated at higher temperatures (eg, see Lundell and Dickey 1977, and Baker et al 1983).

2 Apparatus and experimental procedure

The apparatus developed for this work has been described in detail elsewhere (Hastie et al 1984, 1987) and the essential features are as follows.

2.1 Laser interaction and beam sampling geometry

Figure 1 shows a simplified schematic of the basic technique. Note that the laser, molecular beam orifices, and mass spectrometer are configured to reduce the possibility of laser interaction with the portion of vapor plume directed toward the mass spectrometer. Such an interaction could lead to ionization and plasma effects not characteristic of the vaporization process, as noted in earlier studies, e.g., see Lincoln and Covington (1975). The laser beam enters the continuously evacuated sample chamber at right angles to the mass spectrometer beam line, as shown in figure 1. The minicomputer shown

controls the signal averager and records completed scans of time-resolved mass spectral ion intensities.

After initial test runs at angles varying from 45 to 15 degrees, the angle between the laser beam and sample surface (see figure 1) was chosen as 15 degrees for the data reported here. This geometry represented a compromise between the laser-entrance and mass spectrometer sampling angles. The reduced mass flux for the slightly off-axis sampling was not expected to be significant, as shown by the earlier study of Covington et al (1977). From post-run examination of deposit patterns around vacuum chamber apertures, the vapor plume-to-sample surface orientation was found to be approximately independent of the laser incidence angle. The plume axis was normal to the surface to within a few (~ ± 5) degrees for sample-surface to laser-beam angles ranging from 45 to 15 degrees.

Sample positioning in real-time is achieved by a computer controlled kinematic two-dimensional stage. This stage permits laser-vaporization either from an essentially fresh surface with each pulse or from a selected single spot.

2.2 Laser system

The laser system basically consists of an externally mounted Nd/YAG pulsed laser (10 or 20 Hz frequency using two individual lasers), which operates at several discrete wavelengths from 1060 nm to 350 nm. Earlier studies, for instance those of Ohse et al (1979), Lincoln and Covington (1975) and Olstad and Olander (1975), have indicated the utility of short pulse time, high power lasers (e.g., Nd/YAG) for controlled surface vaporization studies. To allow for ready visual alignment of the beam, the 532 nm doubled line

(green) of the laser fundamental was chosen as the working wavelength for the present studies. The laser pulse times used were in the range 7-20 ns, which convert to thermal pulses of < 100 ns. This time scale is negligible compared to that for the vaporization and beam-transit process (> 100 μs). The laser beam was focused onto the sample by a 500 mm focal length lens, mounted on a stepper motor-driven stage. Sample surface spot sizes of about 250 μm diameter were used and the laser was maintained at a fixed power level for each multi-pulse data-averaging series.

2.3 Sample preparation

The sample mounts used were constructed either of stainless steel or tantalum. Samples were taken from two sources: (1) a rod of spectroscopic grade polycrystalline graphite, selected by the NBS Center for Analytical Chemistry for spectrographic analyses on the basis of its freedom from contaminants; (2) a rod of medium-grain dense graphite similar to HLM grade. The hydrogen content is unknown but is probably insignificant although relatively weak mass spectrometric signals were observed corresponding to C_2H_2 and other low hydrogen-content hydrocarbon gas species. Possible hydrocarbon contributions to the C_n^+ (n = 1 - 9) ion signals are estimated to be less than a few percent and can be neglected. Sample preparation consisted of parting-off a short section of a 1/4 inch (6.4 mm) rod, and milling a flat of the desired angle using carefully cleaned steel cutting tools.

2.4 Vapor plume formation, beam sampling, and analysis procedures

According to Afanasev and Krokhin (1967), at flux densities above about 10^8 W/cm^2 the laser interaction mechanism changes from a thermally controlled

vaporization process to one where thermal pressure ejects material into the laser plasma. However, this theoretically-based argument is for a general case, ie non-material specific. For the highly refractory materials of graphite and BN (reported on elsewhere, Hastie et al 1987) it is still possible to be within the thermal vaporization regime. No evidence was found for a physical ejection process in the present studies using nominal flux densities of ~ 10^8 - 10^9 W/cm^2. The actual fraction of this incident flux that is absorbed by the sample is not known.

In a typical laser-induced vaporization experiment, a laser fluence of about 20 J/cm^2 is focused to an area of ~ 10^{-3} cm^2. The deposited energy is converted into thermal excitation at the surface and penetrates to a depth of only a few tens of atomic diameters. Rapid vaporization occurs, leading at peak-temperature to the formation of a gas-dynamically stabilized plume. The visible region of the plume extended about 1 cm into the first vacuum chamber. This plume undergoes rapid free-jet expansion to yield a collisionless gas stream and a molecular beam. The molecular beam is collimated by three circular, differentially pumped, apertures (not all shown in figure 1), and travels a distance of 26 cm between the sample surface and mass spectrometer ionization chamber. This distance effectively determines the time scale of the measured time-resolved ion-intensity profiles as the transit time in the quadrupole mass filter is negligible. Each aperture is sized to just allow clear passage of the beam through the 4.8 mm diameter entrance aperture of the quadrupole mass filter ion source and, hence, also through the larger (8 mm) ion source exit aperture.

Species are ionized by electron impact at adjustable electron energies, and mass analyzed by the quadrupole mass filter. In the present work, most of the data were obtained with 26 eV ionizing electron energy. This is about 15 and 10 eV above the molecular and dissociative ionization thresholds, respectively. These mass selected ions are then collected and amplified by an electron multiplier. The signals are averaged using 5 μs/channel dwell time, with the sweep synchronized by a trigger generated from the onset of each laser pulse or from the flash lamp. This data-collection procedure gives a time-resolved mass spectral ion-intensity profile of an individual pre-selected mass peak. We designate the profiles as time-of-arrival curves, abbreviated as TOA. Sufficient signal time-sweeps are collected (typically between 100 and 1000) to provide reasonably good statistics in the leading edge and peak centroid area. The data-collection process is repeated for each individual mass peak selected. For a fixed sample spot position it was observed that, dependent on the laser beam to surface angle, the initial signal intensity would decay during the first few tens of pulses and then stabilize at a value about half that produced by the initial pulse. For this reason, each series of intensity-time profiles (for individual masses) was collected after a pre-conditioning period, and successive series were taken from a new spot on the surface. To check for possible changes in laser flux for a number of laser shots, a major peak (eg C_1 or C_3) was sampled both at the beginning and end of a data-collection series.

3 Results and discussion

3.1 Vapor species assignment

Table 1 summarizes the species detected, in the form of singly charged positive ions, by mass spectrometric analysis of the graphite laser plume with 26 eV ionizing electron energy. No higher molecular weight species were detectable. Particular attention was given to the detection of C_{11} which is known to be a prominent species under non-equilibrium cluster-forming conditions (eg, see Rohlfing et al 1984). The absence of detectable C_{11}, or other species at $n > 9$, is indicative of the likelihood of the sampled beam having a frozen equilibrium composition representing that at the vaporizing surface.

For the two representative data sets given in table 1; A was obtained under a static (stationary sample) mode condition, and B under a dynamic mode where the sample was moving continuously, thereby providing to a new vaporizing surface location about every 20 shots. About 3000 laser shots were used for each species in set A, thereby creating a crater of similar dimensions (~ 250 μm diameter) to those produced in an earlier study on BN (Hastie et al 1987). For set B, 1000 shots per species were used across the surface without detectable crater formation. Two different graphite supply sources, commercial laser systems, fluence levels, and focus conditions were used to obtain data-sets A and B. At the sample surface, the laser fluence levels were estimated to be in the range of 20-30 mJ.

During initial heating, hydrocarbon impurities were observed for data-set A. Similar observations have been made by other workers, eg, see Zavitsanos and Carlson, (1973). In the present study, this effect was observed primarily in the form of C_2H^+ (25 amu), $C_2H_2^+$ (26 amu), and $C_4H_2^+$ (50 amu) mass

spectral ions during the initial first few laser shots onto a fresh surface location. These signals tended to vanish, with an increasing number of laser shots, much more rapidly than those for the C_n species, suggesting the presence of surface hydrocarbon contamination. The acetylene species (C_2H_2) was the dominant impurity. It is perhaps pertinent that laser heated graphite in the presence of hydrogen or ethylene also produces acetylene as the major product (Taki et al 1969).

Of particular note was the long TOA for the 26 amu (C_2H_2) species, as compared with the C_n ions. A similar effect can be noted in the results of Lincoln (1969). For comparison, both our data and Lincoln's show a time difference between 26 and 36 amu of 150 to 200 μs. This time delay could result from a number of factors, including the $C_2H_2^+$ arising from electron impact fragmentation of a heavier polyacetylene precursor (the delay implies a species of 110 ± 15 amu), a reaction time such as diffusion in the substrate, or a different degree of gas-dynamic cooling for C_2H_2 as compared with C_n. The 57 amu ($C_4H_9^+$) ion showed an even larger time-delay and the TOA profile was exceptionally wide.

3.2 Vapor species abundance

The relative ion intensities listed in table 1 are believed to be a good indication of the relative species partial pressures. That is, species-dependent electron impact fragmentation and mass spectral sensitivity factors can be neglected to a first approximation, with an estimated uncertainty of 30% in the relative partial pressures. More precise partial pressure data cannot be obtained as no ionization cross section (σ) information exists for any of the polyatomic C_n species. However, various estimates suggest a

gradual increase in σ with n. Under our experimental conditions this trend is compensated for by the known (calibrated) decrease in the quadrupole mass filter transmission efficiency with increasing mass. A potentially more serious source of error in relating ion intensities to partial pressures arises from possible electron impact fragmentation which would enhance lower molecular weight ions at the expense of heavier parent ions. At the 26 eV electron energies used this effect should not be too large. Examination of the TOA profiles indicated no significant (< 20%) ion intensity contributions from fragmentation of heavier ions. Further discussion of the fragmentation question is given in later sections.

Typical TOA profiles, from which integrated ion intensity data are obtained, are given in figures 2 - 4 for data-set B. Similar TOA profiles were obtained for the C_1 - C_5 species of data-set A but with lower sensitivity. The TOA profiles at half-height (0.5 I max) were wider and the peak-intensity times were systematically shorter for set A. Both of these TOA features are indicative of a faster but cooler (narrower velocity distribution) beam for set A compared with set B. This, in turn, indicates a higher sample pressure and surface temperature for data-set A. Future development of a deconvolution model is planned to extract temperature information from the TOA profiles which are somewhat delayed and broadened by the electronic (RC) system time constant (~ 100 - 200 μs).

Ion intensities were computed from the TOA profiles (eg, figures 2 - 4) by two methods. The first used the peak maximum at the peak centroid, and the second used the integrated peak intensity. Both approaches gave consistent relative intensity results which were almost independent of ionizing electron energy at 26 and 96 eV.

Under carefully controlled conditions, the data were very reproducible. However, as seen by the significant difference between data-sets A and B (table 1), the data are sensitive to experimental conditions. With fixed laser conditions, the following factors were found to affect the absolute and relative intensities: sample-type (A and B were from different graphite supply sources), surface morphology (flat or cratered), and surface-heating history. At present, it is not possible to isolate and quantify these effects though future systematic work is planned. For data-set A, the initial intensities resembled those of set B and as a crater developed the intensity variations stabilized to the level shown by set A. We believe that this set most reasonably represents the equilibrium thermodynamic distribution of C_n species partial pressures. Non-equilibrium effects, such as non-unity accommodation coefficients and impurities, are less likely from a pre-heated crater source.

The intensity-time profiles from C_n (e.g., see figures 2-4) are quite similar to those observed in analogous measurements by Olstad and Olander (1975) for Fe_n species. These authors provide a theoretical analysis of the atom density pulses in terms of an equilibrium vaporization model with known laser pulse energy-time profiles. A similar analysis should be possible for the C_n system. However, in the present case the time-scales of the thermal pulse and the TOA profiles are not expected to overlap.

The validity of the assignment of ions to neutral precursors was borne out by the observation of insignificant changes in ion ratios from 26 to 96 eV ionizing electron energy. However, this is only a necessary but not sufficient proof of ion assignment. Additional, more compelling, evidence for the lack of significant electron impact fragmentation is given by the TOA data discussed below (Section 3.3.1).

Comparison, in table 1, of the present ion intensity data with the JANAF (1971, 1985), Livermore (Leider et al, 1973) and Russian (Gurvich et al 1979) literature data for relative partial pressures and the ion intensity data of Zavitsanos(1968) and Berkowitz and Chupka (1964) indicates a much closer agreement with JANAF (1971, 1985) than with the other data sources. The only significant discrepancy between the present results and JANAF (1971, 1985) occurs for the C_1 species when formed under a non-cratered condition (set B in table 1), which is discussed in more detail below. However, the present C_1 results (data-set B) are in satisfactory agreement with those of Berkowitz and Chupka (1964) but C_5 is not in agreement. In fact, no two data-sets show agreement for C_5 for reasons yet to be determined. In this connection, it is noteworthy that the Russian tables (Gurvich et al 1979) recommend a much higher partial pressure for C_5 than observed by us, or others, with the exception of the Zavitsanos (1968) data. It is probably significant that in a subsequent study Zavitsanos and Carlson (1973) were unable to obtain data on C_5 owing to the presence of a large background peak at 60 amu.

Based on the good agreement between the present results and those of JANAF (1971, 1985), we can argue that the C_n (n = 2 - 5) plume species are most likely in local thermodynamic equilibrium and that the graphite species vaporization coefficients appear to be at or near unity. Other significant causes of data-differences between this and earlier work may arise from our efforts to minimize laser/plume interactions and our use of very short laser pulses to reduce perturbation of the gas-dynamic process. Also, as the present study was performed off the central plume axis, it is possible that if non-equilibrium effects occurred only along the perpendicular axis they would

not have been observed in the present work. As the plume is highly forward-peaked in the perpendicular direction this possibility needs further study.

3.3 Temperature determination

For these initial studies, several indirect methods, summarized in table 2 for data-set A, have been used to determine a temperature (T_o) of 4100 ± 200 K for the laser heated spot. For data-set B, using similar methods, the T_o value was determined to be 3800 ± 300 K. Similar methods were used with very satisfactory results for the BN studies described elsewhere (Hastie et al 1987). Application of potentially more accurate optical pyrometric methods have been deferred due to uncertain emissivity data and the difficulty of accounting for plume contributions to the emission signals. Also conventional pyrometric systems do not have the time response needed. Under the laser pulse conditions used, it is likely that only the surface layer (a few wavelengths, i.e., ~ 2000 to 5000 nm) is heated directly and the total extent of vaporization is confined to an area nearly equal to that of the laser spot (Hall 1984).

3.3.1 Beam velocity analysis

The TOA profiles of the beam species may be used to obtain the post-expansion plume temperature. The time position (usually at peak intensity) may be taken as an indication of the group velocity and the profile-shape is characteristic of the velocity distribution. The corresponding temperatures do not necessarily have the same value for gas-dynamic beams. However, regardless of the model used to describe the vaporization and beam-forming process, if a collection of gas molecules is in thermal equilibrium their

velocity function is proportional to $(T/M)^{\frac{1}{2}}$, where M is the individual species molecular weight and T is the post-expansion molecular beam vapor species temperature ($< T_o$). This relation follows from the equipartitioning of translational energy, established under thermal equilibrium conditions, where

$$Mv^2/2 = 3kT/2,$$

and v is the root-mean-square (average) velocity, which is proportional to the most probable velocity, ie, the peak of the thermal velocity distribution, and k is the Boltzmann constant. Identification of the peak location of the observed TOA profile is affected by the noise level. Hence <u>relative</u> TOA values were selected at the half-height position of the leading edge of the TOA profile. Correlating this time ($t_{\frac{1}{2}}$) with the most probable velocity yields the time-of-arrival function

$$t_{\frac{1}{2}} \alpha (d/3kT)^{\frac{1}{2}} \cdot M^{\frac{1}{2}},$$

where d is the flight distance, 26 cm. Hence a linear plot of $t_{\frac{1}{2}}$ versus $M^{\frac{1}{2}}$ is indicative of thermal equilibrium. Figure 5 shows that the various C_n species exhibit such behavior. The linearity of the curves in figure 5 is also excellent evidence for the correct assignment of ions to molecular precursors of the same mass. It should be noted that the zero-mass time intercept (in figure 5) has no physical significance here, owing to the use of half-height TOA's and the affect of the RC time constant on the experimental TOA's.

Further support for thermal equilibration among the various C_n species can be derived from the widths (half-height Δt) of the TOA profiles, such as

those given in figures 2-4. For a common species temperature, it follows from the above discussion that Δt (half-height) is proportional to $M^{\frac{1}{2}}$ and this was generally found to be the case.

In general, the TOA profile curve shapes appear to follow Maxwell-Boltzmann distributions characteristic of a cooled beam. Further, more-detailed, analysis of this preliminary observation will be pursued in future work when the instrumental RC time-delay effects are quantitatively analyzed. It is noteworthy that the TOA peaks do not exhibit the unusual shoulders or splitting present in the C_1 and C_3 profiles obtained by Milne et al (1972) under Knudsen effusion conditions (~ 2700 K beam temperature). These authors attributed these anomalous effects to ion source time-delay effects, including trapping and back-reflection of neutrals into the source. At 50 eV ionizing electron energy, their C_3 TOA profile showed the expected distribution, indicating an absence of fragmentation. However, the C_1 and C_2 TOA profiles did show a broadening at 50 eV, as compared with 17 eV, which was believed to arise from fragmentation of C_3^+ by separate reaction channels to C_1^+ and C_2^+ (< 40% contribution to C_1^+). In the present study, with beam temperatures of < 750 K (produced by gas-dynamic cooling), no broadening of TOA profiles occurred when the electron energy was increased from 26 to 96 eV. However, some broadening of the C_1 TOA profile was noted during the first few laser shots at a fresh surface which could arise from impurity fragmentation. The TOA profiles will be further examined for evidence of secondary effects when the RC time-delay component is eliminated.

From the slope of the data-set A curve in figure 5, we obtain an apparent beam temperature of 1100 ± 200 K. Correction for the time difference factor (empirical value = 0.68) between $t_{\frac{1}{2}}$ and the peak-intensity time gives a beam

group temperature of 750 ± 200 K. This value is an upper limit as it is affected by the instrumental RC time-delay. However, it is consistent with the cooling affect expected from the isentropic free-jet expansion process. Comparison of this value with that obtained similarly for the BN system (670 K) (Hastie et al 1987), together with the BN surface temperature of 2900 K, indicates a graphite surface temperature of 3300 ± 600 K. We expect to improve the accuracy of this determination when the instrumental (RC-delay) contribution to the TOA profiles is established. Direct comparisons of individual TOA curves provide more accurate temperatures. For instance, by comparing the relative C_2^+ arrival time with that for B_1^+ at T_o = 2900 K (Hastie et al 1987) we obtain a graphite surface temperature value of 4000 ± 300 K, which is in good agreement with other temperature indicators (see table 2).

The relative beam temperatures for data-sets A and B, obtained from the curve slopes in figure 5, indicate about an order of magnitude lower source pressure for data-set B. That is, for the conditions of data-set B, there is less gasdynamic acceleration of the beam due to the lower source pressure. This difference in source pressure is consistent with the difference in source temperatures for the two data sets.

3.3.2 Temperature from partial pressure determination

Independent evidence for a pre-expansion (and hence surface) temperature in the region of 4100 K is provided by the absolute partial pressure, P_i, data. The relationship between P_i and the integrated ion intensities, I^+, for species i is given by

$$P_i = kI^+T,$$

where k is a constant determined by vaporization of a calibrant material at known pressure and temperature. A calibration was performed using the well established NaCl system with the same mass spectrometer and molecular beam-path conditions. The graphite gas-dynamic conditions were simulated by use of transpiration mass spectrometry to produce a supersonic expansion of NaCl in N_2 (Bonnell and Hastie 1979). The value of k obtained was adjusted for the C_1 case using the known ionization cross section (σ) differences between NaCl (Bonnell and Hastie 1979) and C_1 (Mann 1969) at the 26 eV ionizing electron energy used (σ_C / σ_{NaCl} = 1.6). With this approach, we find

$$P_C = 0.1 \text{ atm}$$

for data-set A of table 1. A similar result is obtained if one compares the σ-adjusted ion intensities of C_2^+ and B_1^+ (Hastie et al 1987). For an equilibrium condition with the JANAF (1971, 1985) thermodynamic functions, this partial pressure corresponds to a temperature of 4100 $\pm$ 200 K. The error represents the temperature span over which P_C changes by a factor of 3, which we consider a conservative estimate of the probable uncertainty in the derived P_C. For the data in table 1, the sum of the individual species partial pressures is in the region of 1.0 atm, the sublimation pressure of graphite. It also follows that the species detectability limit for the present experimental conditions was ~ 10^{-4} atm. If one considers the source pressure of 1 atm this sensitivity value is much lower than normal for high temperature mass spectrometry. However, the free-jet expansion process produces a gas of final expansion pressure in the region of ~ 10^{-5} atm. Hence the 10^{-4} atm detectability limit effectively refers to this 10^{-5} atm source and the sensitivity is then comparable with Knudsen mass spectrometry.

3.3.3 Temperature from species relative intensities

The TOA evidence for thermal equilibrium suggests that the "known" C_n species partial pressure distribution with temperature can be used to infer the sample temperature (T_o) from the measured species concentration ratios. Also, the beam-formation process is quite similar to that for more usual supersonic expansions where the beam composition represents a "frozen equilibrium" which corresponds to the pre-expansion temperature/pressure conditions (Bonnell and Hastie 1979). The high pumping speed of the vacuum system used for the present studies, and the pulsed nature of the gas evolution process, further ensures high expansion ratios and "frozen equilibrium" compositions in the gas-dynamic process.

Values of "known" C_n species concentration ratios were calculated as a function of temperature using JANAF (1971, 1985) and other thermochemical tables (Leider et al 1973, Meyer and Lynch 1973; Gurvich et al 1979). Figure 6 gives the JANAF (1971, 1985)-based data and it is apparent that the C_5/C_3 and C_4/C_3 ratios are the most sensitive temperature indicators. Table 3 gives temperatures calculated from the experimental C_n/C_3 ratio data and it is clear that the most realistic temperature data result from use of the experimental intensity ratios together with the JANAF (1971, 1985) thermochemical data. That is, the Livermore (Leider et al, 1973) and Meyer and Lynch (1973) revisions and reassessments of the earlier JANAF (1971, 1985) thermodynamic functions are not as consistent with the present results. The more recent Russian tables (Gurvich et al 1979) appear to overestimate the importance of C_5 as discussed earlier.

Anomalous C_1 / C_3 behavior: the anomalous low temperature result indicated (in table 3) by the C_1/C_3 ratio for data-set B could be interpreted

as being due either to an apparent excess of C_1 or to a deficiency in C_3. Arguments for and against additional sources of C_1^+ include:

- An excess intensity level of C_1^+ could arise from electron impact fragmentation of higher mass C_n species or of contaminants such as CO or hydrocarbons. In this connection, it should be noted that the literature data were usually obtained at lower electron energies than for the present study. However, the present results are consistent with the lower eV data of Berkowitz and Chupka (1964) and Drowart et al (1959).

- A compelling argument against significant fragmentation in the present study is the Maxwellian form of the TOA profile (figure 5) which indicates that C_1^+ arises primarily from a 12 amu neutral precursor, ie, C_1.

- The fact that the C_1^+ TOA follows the $t_{\frac{1}{2}}$ vs $M^{\frac{1}{2}}$ correlation (figure 5) is also very good evidence for the absence of higher molecular weight species contributing to C_1^+ by electron impact fragmentation.

- Analysis of the C_n^+ ion-stabilities (bond dissociation energies) indicates no loss of stability on ionization of C_n, hence no major fragmentation effect is expected (eg. see Hastie and Margrave 1968, 1969).

- The constancy of ion-ratios over the range 26 to 96 eV is consistent with an absence of fragmentation and suggests the existence of a single ion-precursor for all ions. However, this is not a definitive proof as the fragmentation efficiency may not change between 26 and 96 eV.

- The C_1^+ appearance potential curve was inconclusive with respect to fragment-ion contributions owing to an unusually large tailing near the thresh-hold energy which did, however, agree with that for atomic carbon. This effect requires further study with improved sensitivity.

- Anomalous (and unprecedented) variations in relative ionization cross sections or vaporization coefficients for C_1 or C_3 could also account for some of the observed data, though this is not considered likely.

In summary, the above arguments indicate that the high C_1^+ intensity most likely arises from an anomalously high C_1 concentration. Supporting evidence for this conclusion is provided by the observations of Wachi and Gilmartin (1970) to the effect that the C_1/C_n ratios decreased with time and also depended on the sample preparation and surface morphology. The fact that data-sets A and B (table 1), which show a significant difference in C_1^+ relative intensity, represent two different samples and surface morphologies is also consistent with Wachi and Gilmartins' (1970) observations. Hence the

C_1^+ data do not appear to have thermodynamic significance for C_1 concentration measurement except for the cratered condition used to obtain data-set A.

Another, less-likely, argument as to why C_1/C_3 gives a lower T_o than C_n/C_3 ($n > 1$) is based on the higher sublimation enthalpies for C_n ($n > 1$), than for C_1 (as may be seen from the curve slopes of figure 7). This means that C_1 becomes a relatively more important species at lower temperatures and; as the hot spot cools, C_1 could become relatively more significant than C_n ($n > 1$). However, such an effect should also be manifested in the B_1/B_2 ratio data obtained for the BN system (Hastie et al 1987), and this was not the case.

For the case of the C_2/C_3 ratio (data-set A, table 1), if the relative ionization cross-sections were 1/1.5, which is quite reasonable based on empirical trends in other systems, the calculated temperature of 3400 K would be increased to 4200 K which is in closer agreement with the values obtained using the C_4 and C_5 species. This cross-section ratio agrees favorably with the estimate of 1/1.23 given by Meyer and Lynch (1973). The higher polymeric C_n species ($n > 3$) should have cross-section ratios close to unity, which we have assumed in the present analysis.

Finally, the possibility that C_3 rather than C_1 or C_2 behaves anomalously should be considered. At temperatures less than 2700 K it is known that C_3 has a low vaporization coefficient (α), but this is expected to increase with increasing temperature. Baker and Covington (1982) provide indirect evidence for the average α_n, over all C_n species, to fall in the range of 0.5 - 1.0 at temperatures in the region of 4000 K. In the present experiments, both C_3 and C_2 would need to have α values below this range to account for the observed variations of C_n/C_3. Future measurements of C_n/C_3 as a function of surface

morphology are planned to test for possible non-unity behavior for α_n. However, the present data do not support α_n values of much less than unity. A similar conclusion was also made by Lundell and Dickey (1977), based on CW-laser vaporization studies over the temperature range 4000 - 4500 K. The observed mass-loss rates were also consistent with that predicted from the JANAF (1971, 1985) data using a gas-dynamic model.

4 Summary and conclusions

Laser pulses at 532 nm wavelength, with pulse widths in the range 7-20 ns and power densities in the range of ~10^8 - 10^9 W/cm^2, impacting graphite surfaces at 15-45° incidence angles, produce vapor plumes with total pressures in the range of ~ 0.1 - 1 atm and pre-expansion temperatures between 3800 ± 300 and 4100 ± 200 K. The pre-expansion vapor and surface temperatures were determined by a number of independent, indirect methods. The vapor plumes formed originated either from craters or from a relatively flat surface, depending on the number of laser shots used to obtain data at a fixed sample location. It is believed that the cratered condition more closely approaches equilibrium. Partial pressures were determined for the principal vapor species C_1-C_9.

No significant mass spectral interferences due to electron impact fragmentation were detected. We surmise that the observed isentropic cooling (to < 700 K), which results from plume free-jet expansion into the high vacuum chamber, reduces the normal thermal excitation and the availability of dissociation channels for electron impact fragmentation. In this connection, it is interesting to note the tendency for C_n cluster (ie non-equilibrium)

species to photodissociate according to the reaction,

$$C_n + h\nu = C_{n-3}^+ + C_3$$

(Geusic et al 1986). This process was found to be particularly prominant for $n > 6$ and the driving force can be attributed to the high stability of C_3. It is reasonable to expect similar behavior for electron impact conditions, although the relative abundance of C_n species differs significantly under the non-clustering conditions of the present work. In the present case, we could expect to see the following fragment-ion to neutral precursor pairings:

$$C_1^+ (C_4),\ C_2^+ (C_5),\ C_3^+ (C_6),\ C_4^+ (C_7),\ C_5^+ (C_8),\ \text{etc.}$$

in decreasing order of significance. However, the TOA profiles do not show the presence of any significant (> 20%) high mass shoulders or broadening. For the relatively noisy TOA data corresponding to C_7, C_8, and C_9 it is presently not possible to exclude contributions from higher masses although this is very unlikely because of the reduced thermodynamic significance of $n > 9$ precursor species.

Future use of TOA mass spectral intensity profiles for temperature determination shows promise once instrumental time-delay effects are reduced, or at least quantified, in the present apparatus. Similarly, once an absolute time scale is established for the TOA profiles, their degree of conformity to Maxwell-Boltzmann or other temperature distributions can be investigated. It should also be possible to deconvolute these profiles and provide unique mechanistic information on electron impact fragmentation pathways, temperature-dependent ionization cross sections, cluster formation, and other plume-dynamics phenomena. One of the early suggested explanations for data

inconsistencies in the C_3 thermodynamic functions was, in fact, the possibility of a temperature-dependent σ which would affect both Second and Third Law analyses of vaporization data (attributed to L. Brewer by Liskow et al 1972).

Comparison of the C_n (n = 1-5) species partial pressures with values calculated from the JANAF (1971, 1985) thermodynamic functions is very favorable, particularly for vaporization from a crater. However, the C_5 and C_6 species are much less significant than predicted from the Livermore (Leider et al 1973) thermodynamic functions but the C_7 species partial pressure agrees well with their prediction. Possible sources of error in previous studies include, the presence of hydrocarbon impurities, and low gas-dynamic expansion ratios with the kinetic formation of cluster species. We expect that with further development of the LVMS technique, the uncertainties in partial pressures and temperatures can be significantly reduced and a revision of the thermodynamic functions can be made. However, the present results do not support the arguments of Baker et al (1983) to the effect that the Livermore (Leider et al 1973) functions are more reliable than those for JANAF (1971, 1985).

The C_1 species appeared to be particularly sensitive to the experimental surface conditions, which probably accounts for the lack of reproducibility between various workers. Further systematic study is planned to better define the reasons for the apparently anomalous behavior of C_1, relative to C_3. With this exception, the data suggest the various C_n species to be formed at local thermodynamic equilibrium, even for very short laser heating times.

From the pressure information determined by this approach, one can calculate an approximate rate of mass transport for a given surface area. For the hot spot sizes used, we calculate this rate to be in the region of $\sim 10^{-4}$ gm/s. Using the JANAF (1971) vaporization enthalpy data, it follows that the heating and vaporization process removes only about 10^{-5} Joule per laser pulse from the system. As this energy is several orders of magnitude less than that provided by the laser then it appears that the primary energy loss mechanism is not by vaporization but by conduction through the sample. Work is in progress on development of an energy loss model.

ACKNOWLEDGEMENTS

A.B. Sessoms and M. Wilke have provided valuable technical assistance in the construction and maintenance of the Laser-Induced Vaporization Mass Spectrometry System. Financial support for this work has been provided, in part, by the Air Force Office of Scientific Research. Initial development of the basic multistage vacuum system was supported by the Army Research Office for flame analysis experiments.

REFERENCES

Afanasev Yu V, Krokhin O N, 1967 Soviet Phys. JETP 25, 639.

Arnold W, Kowalski J, Putlitz zu G, Stehlin T, and Trager F, 1986, Z Phys. D - Atoms, Molecules and Clusters 3, 329.

Baker R L, Covington M A, and Rosenblatt G M, 1983 "The Determination of Carbon Thermochemical Properties by Laser Vaporization", in High Temperature Materials II, Eds. Z. A. Munir and D. Cubicciotti (Electrochem. Soc., Pennington, NJ) p. 143.

Baker R L, Covington M A, 1982 The High Temperature Thermochemical Properties of Carbon, Report SD-TR-82-19 (ADA112977, NTIS).

Berkowitz J, Chupka W J, 1964 J. Chem. Phys. 40, 2735.

Bonnell D W, Hastie J W, 1979 in Characterization of High Temperature Vapors and Gases, J. W. Hastie, ed., NBS SP 561, (U.S. Govt Printing Office, Washington, D.C.) p. 357.

Covington M A, Liu G N, Lincoln K A, 1977 AIAA J. 15, 1174.

Drowart J, Burns R P, De Maria G, Inghram M G, 1959 J. Chem. Phys. 31, 1131.

Geusic M E, Jarrold M F, McIlrath T J, Bloomfield L A, Freeman R R, Brown W L, 1986, Z. Phys. D. - Atoms, Molecules and Clusters, 3, 309.

Gurvich L V, Viets I V, Medvedev V A, Khachkurozov G A, Yungman V S, Bergman G A, et al. 1979, "Thermodinamicheskie Svoistva Individual'nykh Veshchestu" (Thermodynamic Properties of Individual Substances); Glushko, V. P., gen. ed., Vol II parts 1 and 2.

Hall R, 1984 Private Communication.

Hastie J W, Margrave J L, 1968 Fluorine Chem. Rev., 2, 77.

Hastie J W, Margrave J L, 1969 J. Phys. Chem. 73, 1105.

Hastie J W, Bonnell D W, Schenck P K, 1987 "Laser-Induced Vaporization Mass Spectrometry of Refractory Materials. Part I, Apparatus and the BN System", High Temp. Sci. in press.

Hastie J W, Bonnell D W, Schenck P K, 1984 "Molecular Basis for Laser-Induced Vaporization of Refractory Materials", NBSIR 84, 2983

Hoch M, Ramakrishnan D, Vernardakis T, 1974, Advances in Mass Spectrometry, vol. 6, A. R. West, ed. (Applied Science, Pub. Essex, U.K.) p. 571.

JANAF Thermochemical Tables, 2nd Ed., NSRDS-NBS 37 (Washington, D.C. 1971) and supplements (e.g., J. Phys. Chem. Ref. Data, 3, 311-480 (1974); 4, 1-175 (1975); 7 793-940 (1978); 11, 695-940 (1982); 14, Supplement 1, 535-681 (1985).

Leider H R, Krikorian O H, Young D A, 1973 Carbon 11, 555.

Lincoln K A, Covington M A, 1975 Int. J. Mass Spec. Ion Phys. 16, 191.

Lincoln K A, 1969 in "High Temperature Technology," (Butterworths and Co., London), p. 323.

Liskow D H, Bender C F, Schaefer III H F, 1972 J. Chem. Phys. 66, 5075.

Lundell J H, Dickey R R, 1977 Progr. Astron. and Aeron, 56, 405.

Lundell J H, 1982 Progr. Astron. and Aeron. 83, 472.

Mann J B, 1969 "Ionization Cross Sections of the Elements," in Recent Developments in Mass Spectroscopy, Ed. K. Ogata and T. Hayakawa, (Univ. Park Press, Baltimore) also, private communication, for cross sections as a function of electron energy, p. 814.

Meyer R T, Lynch A W, Freese J M, 1973 J. Phys. Chem. 77, 1083.

Meyer R T, Lynch A W, 1973 High Temp. Science 5, 192.

Milne T A, Beachey J E, Greene F T, 1972 In "Vaporization Kinetics and Thermodynamics of Graphite Using the High Pressure Mass Spectrometer," AFML- TR-72-227 (AD 753713).

Ohse R W, Babelot J F, Cercignani C, Kinsman P J, Long K A, Magill J, Scotti A, 1979 in Characterization of High Temperature Vapors and Gases, J. W. Hastie, ed., NBS SP 561, U.S. Govt. Printing Office, Washington, D.C.) p. 83.

Olstad R A, Olander D R, 1975 J. Appl. Phys. 46, 1509.

Rohlfing E A, Cox D M, Kaldor A, 1984 J. Chem. Phys. 81, 3322.

Stickley C M, May 15-16, 1985 "Countermeasures Development (LCMMD) Program Review," (The BMD Corp.)

Taki K, Kim P H, Namba S, 1969 Bull. Chem. Soc. Japan 42, 823.

Wachi F M, Gilmartin D E, 1970 Carbon 8, 141.

Zavitsanos P D, 1968 Carbon 6, 731.

Zavitsanos P D, Carlson G A, 1973 J. Chem. Phys. 59, 2

Table 1. Mass Spectral Ion Intensity and Relative Partial Pressure Data (Normalized to C_3) for Laser Vaporized Graphite

Mass (amu)	Species	This Work[a]		JANAF[b]	Livermore[b]	Russian[b]	Berkowitz[b]	Zavitsanos[b]
		A(4100 K)	B(3800 K)	4100 K	~4100 K	4100 K	~4000 K	~4100 K, 20 eV
12	C_1	0.15	0.63	0.11	0.06	0.08	0.37	0.5
24	C_2	0.12	0.22	0.15	0.08	0.13	0.31	1.0
36	C_3	1.0	1.0	1.0	1.0	1.0	1.0	1.0
48	C_4	0.01	0.007	0.012	0.04	0.03	0.02	0.24
60	C_5	0.02	0.008	0.027	0.1	0.19	0.08	0.4
72	C_6	c	0.001	-	0.01	-	0.004	0.13
84	C_7	c	0.003	-	0.03	-	0.01	0.16
96	C_8	c	0.002	-	-	-	0.002	0.12
108	C_9	c	0.001	-	-	-	0.001	0.13

[a] From integrated signals between 0 and 2.5 ms for TOA profiles such as those given in figures 2-4. See text for definitions of data sets A and B.

[b] See text for literature citations. JANAF, Livermore, and Russian data are relative partial pressures normalized to C_3, where the absolute C_3 partial pressures are 0.91 and 1.32 atm for the JANAF and Russian data, respectively, for instance.

[c] Not recorded due to low sensitivity.

Table 2. Surface Temperature Results in the Graphite System (Data-Set A)

Method	Temperature (K)
C_2^+ arrival time relative to B_1^+ at 2900 K)	4000 ± 300
P_C from $P = k\, I(C_1^+)\, T$, with JANAF (1971)	4100 ± 200
C_1^+/B_1^+ intensity ratio (for B at 2900 K)	4000 ± 300
C_2^+/B_1^+ intensity ratio (for B at 2900 K)	3900 ± 300
C_4^+/C_3^+ intensity comparison with JANAF (1971)	4000 ± 300
C_5^+/C_3^+ intensity comparison with JANAF (1971)	3900 ± 300
Selected Value =	4100 ± 200

Table 3. Temperatures (K) Calculated from Partial Pressure Ratios, Relative to C_3, (as Listed in Table 1 for Data-Sets A and B) for Various Thermochemical Data Sources

Species	JANAF (1971)		Livermore (Leider et al. 1973)		Meyer and Lynch (1973)	Gurvich et al. (1979)	
	A	B	A	B	A	A	B
C_1	3600	2300	~0	~0	>3500	2500	3200
C_2	3400	4700	>5000	∞	3500	4000	4600
C_3	-	-	-	-	-	-	-
C_4	4000	3700	3300	3100	>5000	3600	3300
C_5	3900	3500	3200	3100	>5000	3100	2700

Captions

Figure 1 Schematic of laser-induced vaporization mass spectrometric facility (side-sectioned view), showing laser-sample-molecular beam geometries.

Figure 2 Mass spectral TOA profiles (scaled to unit intensity) for the C_1^+, C_2^+, C_3^+ species produced by 26 eV ionizing electron energy. Relative peak ion intensities are 2.4, 2.1, and 3.4 respectively. The time-scale has been corrected for the 180 μs laser pulse initiation time. Note that the curves connect data points taken every 500 μs.

Figure 3 Mass spectral TOA profiles (scaled to unit intensity) for the C_4^+, C_5^+, C_6^+ species produced by 26 eV ionizing electron energy. Relative peak ion intensities are 0.9, 0.6, and 1.3 respectively. Other conditions similar to figure 2 (see caption).

Figure 4 Mass spectral TOA profiles (scaled to unit intensity) for the C_7^+, C_8^+, C_9^+ species produced by 26 eV ionizing electron energy. Relative peak ion intensities are 0.5, 0.5, and, 0.1 respectively. Other conditions similar to figure 2 (see caption).

Figure 5 Dependence of the half-height TOA values for C_n (n = 1 to 5 or 9) ions as a function of molecular weight (square root). The circular and square data points are for data-sets A and B, respectively, obtained at 26 eV. The time-scales have been corrected for the non-zero time of the laser pulse initiation, ie 60 μs and 180 μs for data-sets A and B, respectively.

Figure 6 Comparison of experimental (data set A, table 1) and JANAF (1971, 1985) predicted C_n species partial pressure ratios at 4100 K.

Figure 7 Comparison of experimental (data-set A, table 1 for C_1-C_5 and B for C_6-C_9) and JANAF (1971, 1985)-predicted partial pressure versus reciprocal temperature data for C_n (n = 1-9) species.

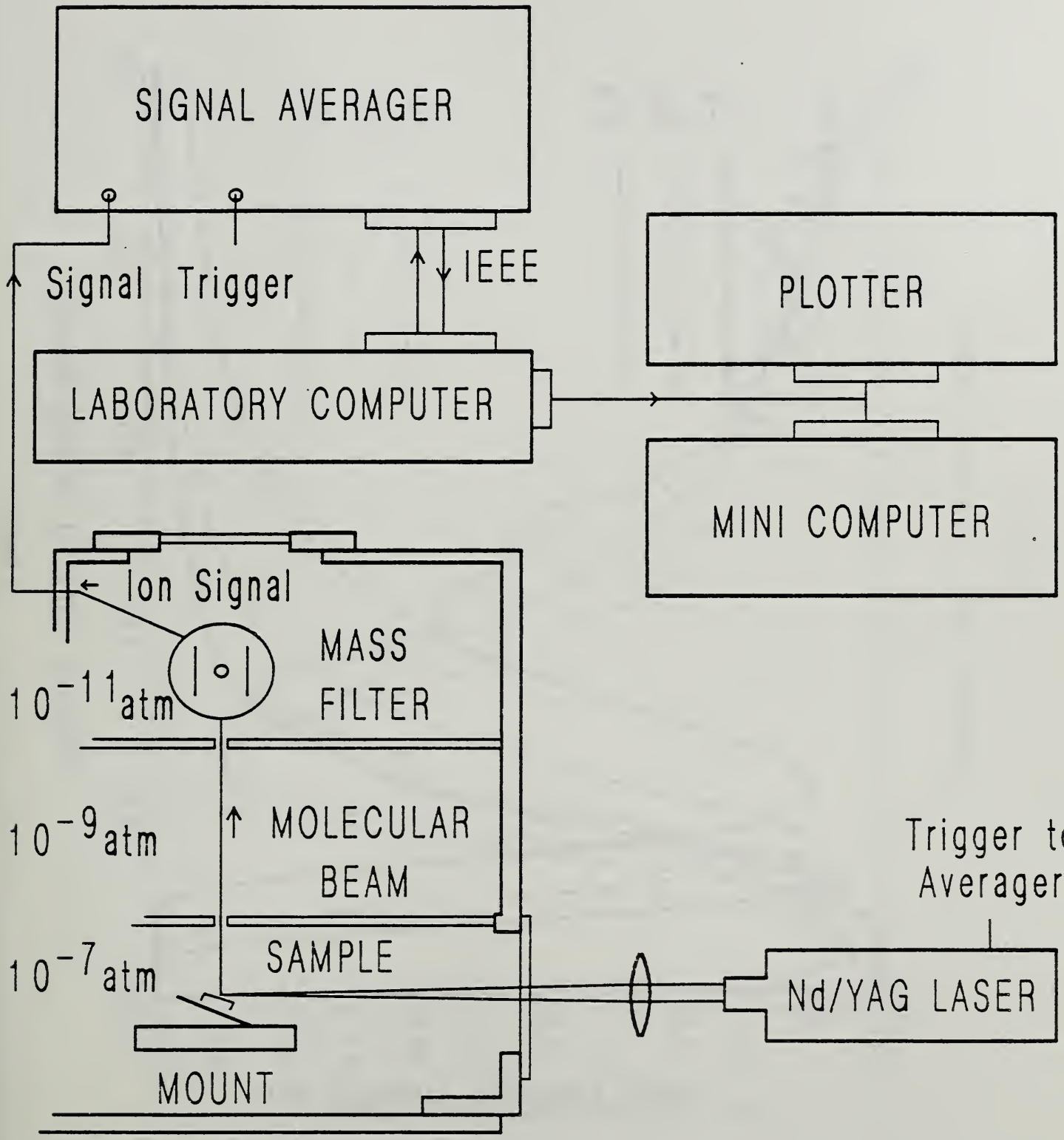
SIGNAL AVERAGER
Signal
Trigger
IEEE
PLOTTER
LABORATORY COMPUTER
MINI COMPUTER
Ion Signal
MASS
FILTER
10^{-11}atm
10^{-9}atm
MOLECULAR
BEAM
Trigger to
Averager
SAMPLE
10^{-7}atm
Nd/YAG LASER
MOUNT

Figure 1

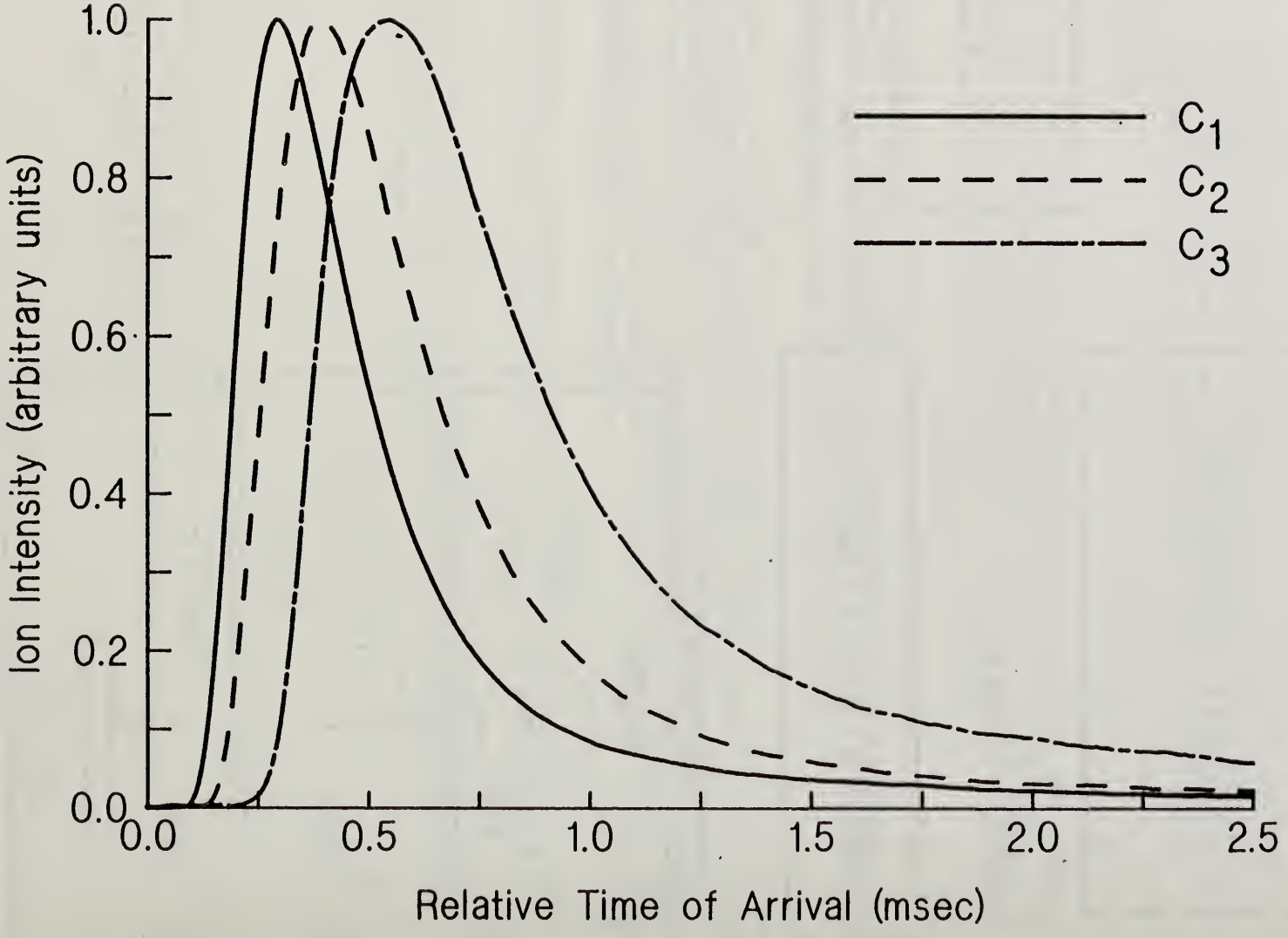
1.0
0.8
0.6
0.4
0.2
0.0
Ion Intensity (arbitrary units)
0.0
0.5
1.0
1.5
2.0
2.5
Relative Time of Arrival (msec)
C1
C2
C3

Figure 2

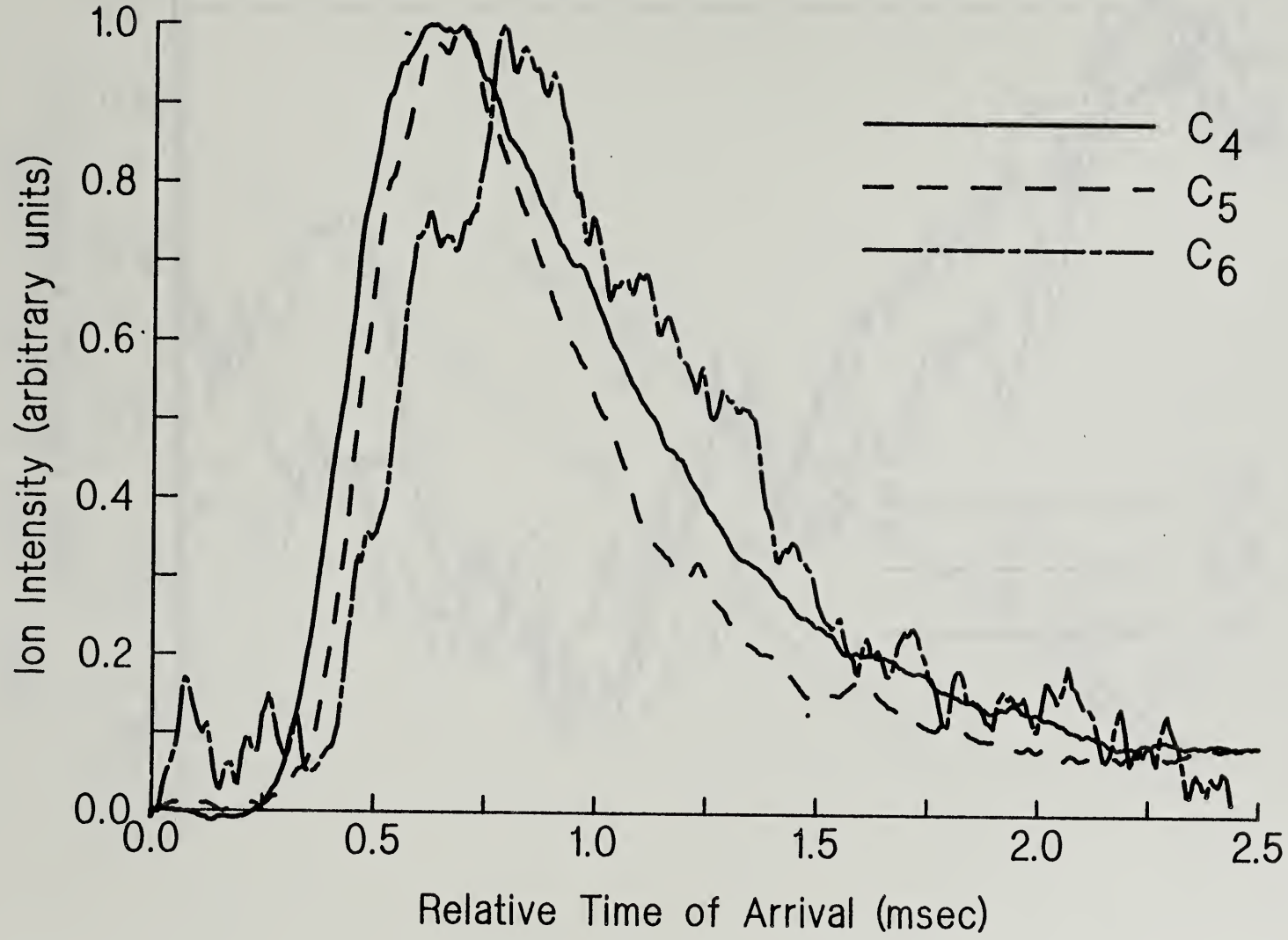
1.0
0.8
0.6
0.4
0.2
0.0
Ion Intensity (arbitrary units)
0.0
0.5
1.0
1.5
2.0
2.5
Relative Time of Arrival (msec)
C4
C5
C6

Figure 3

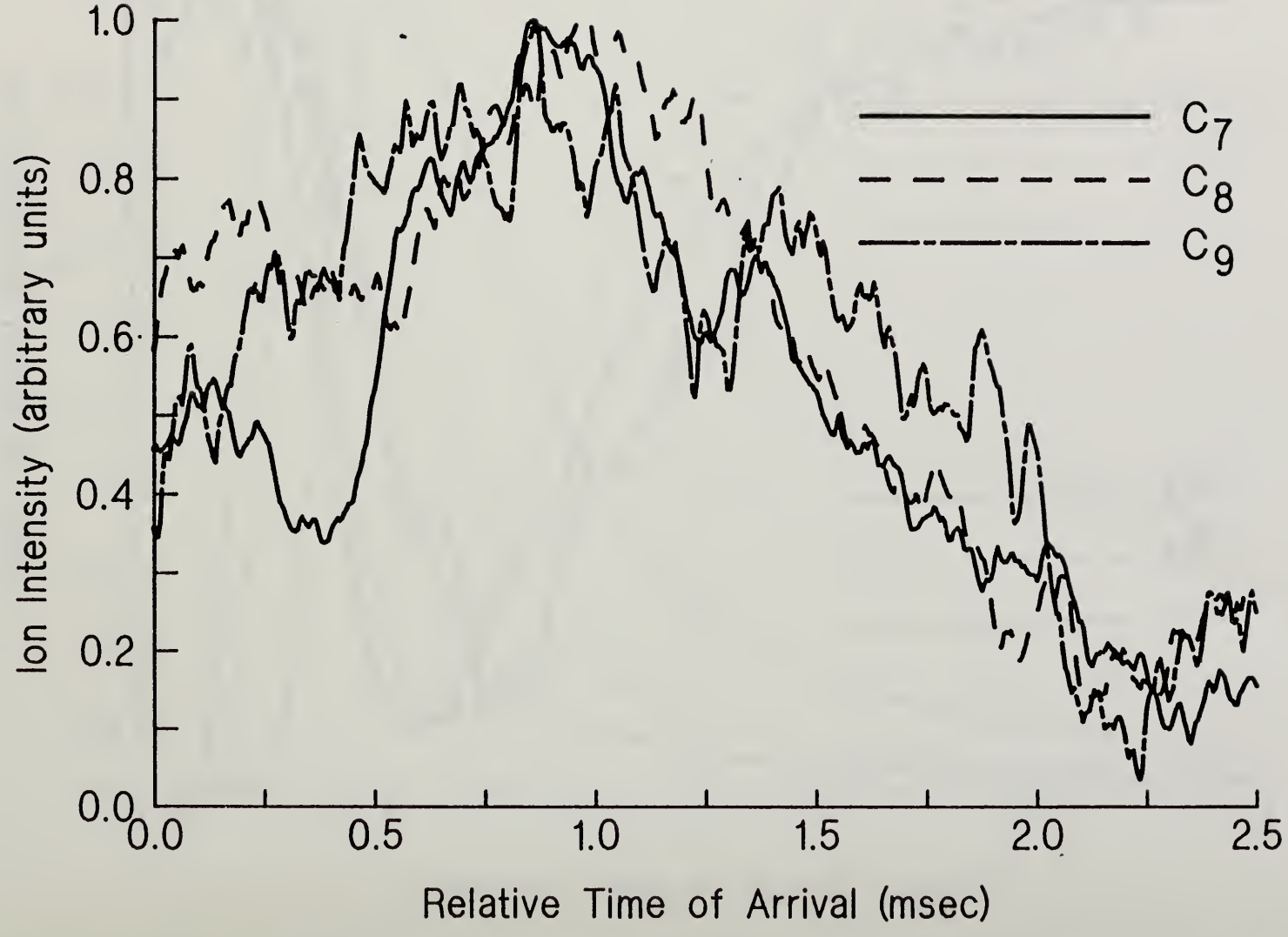
1.0
0.8
0.6
0.4
0.2
0.0
Ion Intensity (arbitrary units)
0.0
0.5
1.0
1.5
2.0
2.5
Relative Time of Arrival (msec)
C7
C8
C9

Figure 4

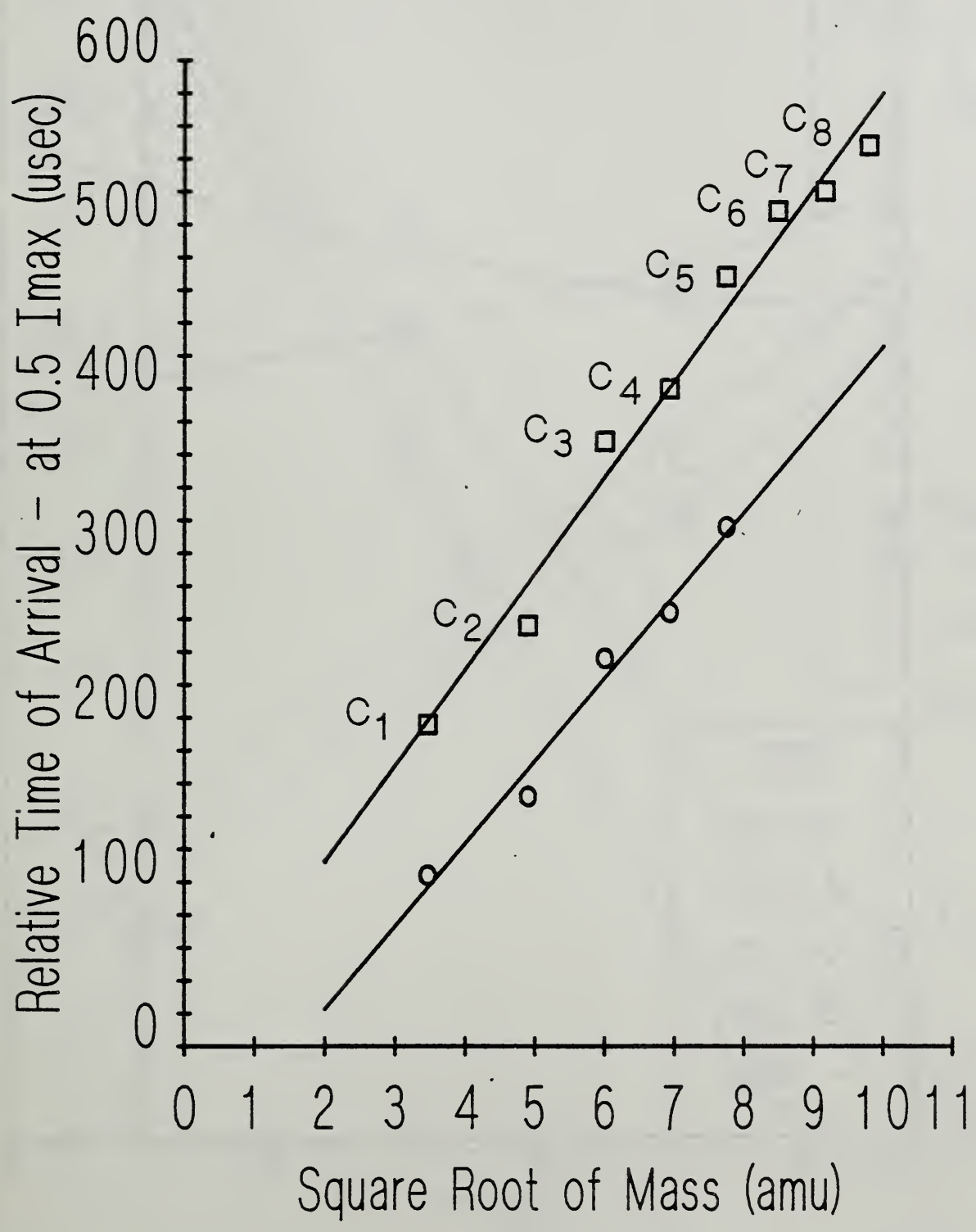
Relative Time of Arrival - at 0.5 Imax (usec)
600
500
400
300
200
100
0
0 1 2 3 4 5 6 7 8 9 10 11
Square Root of Mass (amu)
C1
C2
C3
C4
C5
C6
C7
C8

Figure 5

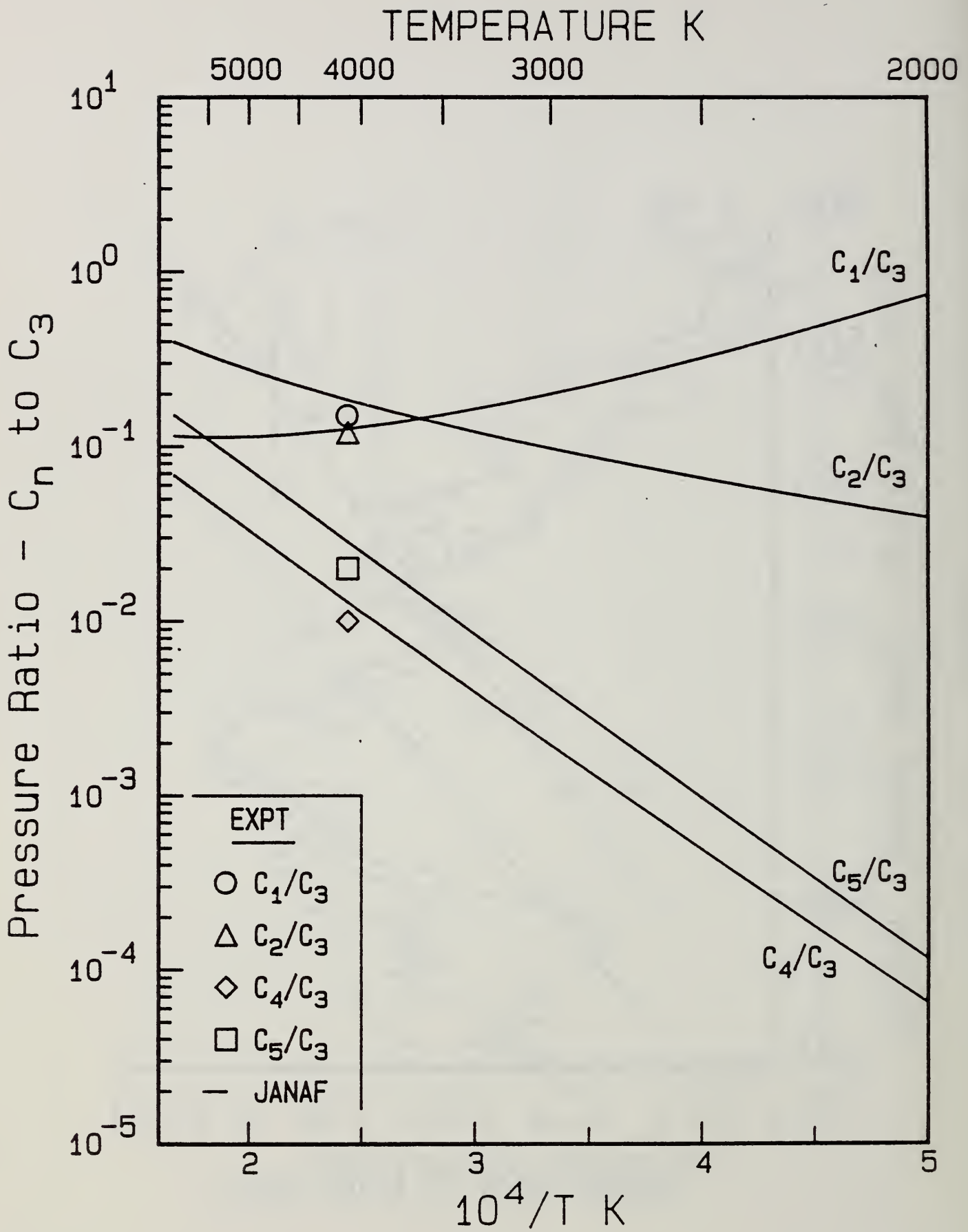
TEMPERATURE K
5000
4000
3000
2000
10^{1}
10^{0}
10^{-1}
10^{-2}
10^{-3}
10^{-4}
10^{-5}
Pressure Ratio - C_n to C_3
C_1/C_3
C_2/C_3
C_5/C_3
C_4/C_3
EXPT
C_1/C_3
C_2/C_3
C_4/C_3
C_5/C_3
JANAF
2
3
4
5
$10^4/T$ K

Figure 6

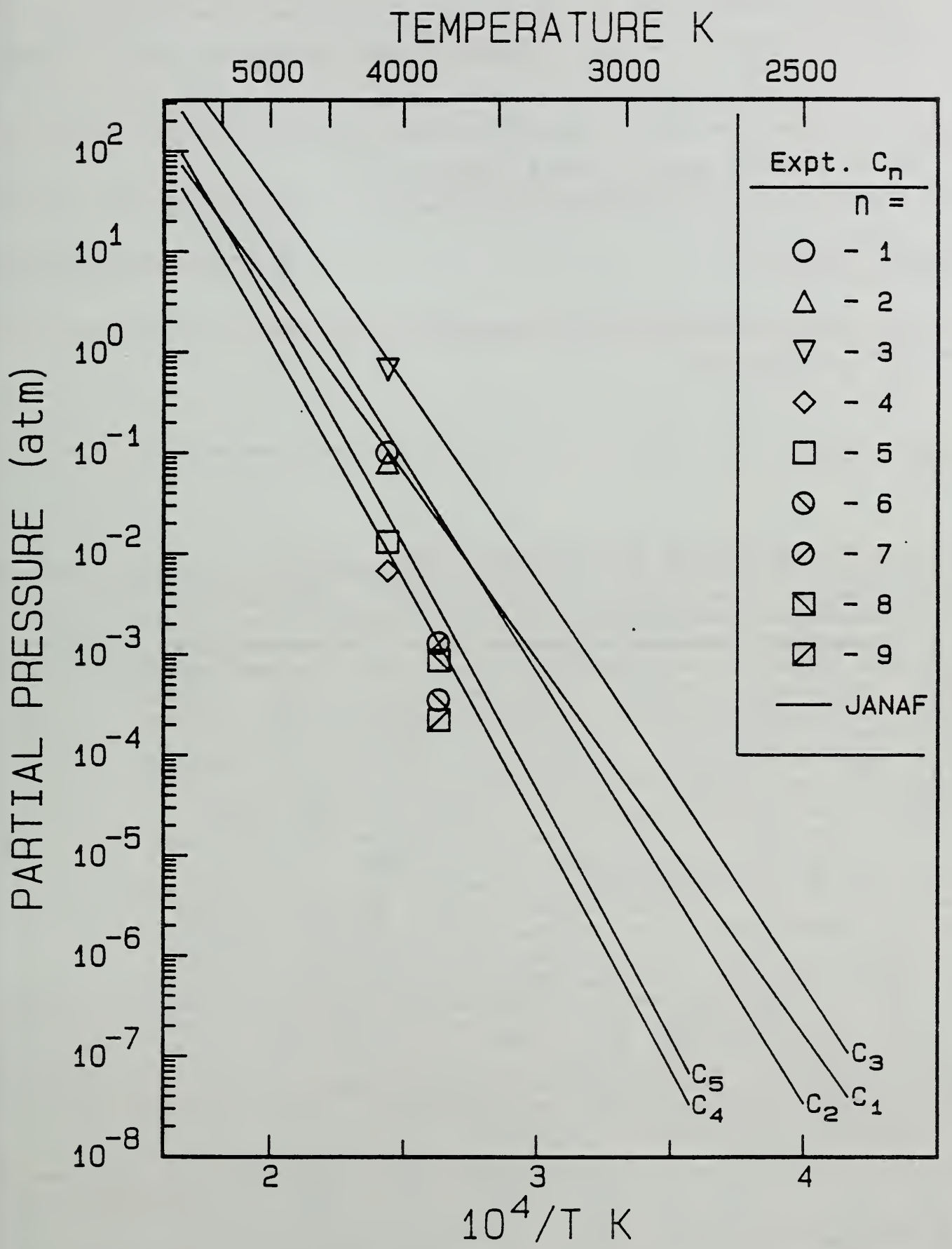
TEMPERATURE K
5000
4000
3000
2500
PARTIAL PRESSURE (atm)
10^{2}
10^{1}
10^{0}
10^{-1}
10^{-2}
10^{-3}
10^{-4}
10^{-5}
10^{-6}
10^{-7}
10^{-8}
2
3
4
$10^{4}/T$ K
Expt. C_n
n =
1
2
3
4
5
6
7
8
9
JANAF
C_3
C_1
C_2
C_5
C_4

Figure 7

NBS-114A (REV. 2-8C)

U.S. DEPT. OF COMM. BIBLIOGRAPHIC DATA SHEET (See instructions)	1. PUBLICATION OR REPORT NO. NBSIR 87-3561	2. Performing Organ. Report No.	3. Publication Date MAY 1987

4. TITLE AND SUBTITLE

Thermochemistry of Materials by Laser Vaporization Mass Spectrometry, Part II Graphite

5. AUTHOR(S)

John W. Hastie, David W. Bonnell, Peter K. Schenck

6. PERFORMING ORGANIZATION (If joint or other than NBS, see instructions)

NATIONAL BUREAU OF STANDARDS
DEPARTMENT OF COMMERCE
WASHINGTON, D.C. 20234

7. Contract/Grant No.

8. Type of Report & Period Covered

9. SPONSORING ORGANIZATION NAME AND COMPLETE ADDRESS (Street, City, State, ZIP)

National Bureau of Standards
Gaithersburg, MD 20899

10. SUPPLEMENTARY NOTES

☐ Document describes a computer program; SF-185, FIPS Software Summary, is attached.

11. ABSTRACT (A 200-word or less factual summary of most significant information. If document includes a significant bibliography In an earlier study (Part I of this series) an experimental approach which couples laser heating of refractory materials under vacuum with mass spectrometric detection of the vapor plume, for thermochemical determinations, of 2900 K was demonstrated using the BN refractory system at 2900 K. This paper describes the results of a similar study on graphite at temperatures around 4100 K and total species pressures in the vicinity of an atmosphere (1 atm = 1.01325×10^5 Nm^{-2}). A Nd/YAG laser system, focused to power densities in the range of 10^9 - 10^{10} W/cm^2, was found to be a convenient energy source for producing controlled vapor plumes and with negligible post-vaporization perturbation of the neutral species identity and concentration. The principal vapor species were found to be C_n (n = 1 - 9) and their relative intensities were found to be more consistent with the JANAF Thermochemical Tables than more recent literature assessments and results. No means were available to directly determine surface temperatures under the experimental conditions of very short heating times (7 - 20 ns) and luminous vapor plumes. Therefore various indirect methods were used, including comparison of the total and partial pressure data with literature results and time-of-flight analysis of the plume species. Surface temperatures were found to be in the region of 4100 ± 300 K and the sum of the C_n species partial pressures was determined to be in the vicinity of 1 atm.

12. KEY WORDS (Six to twelve entries; alphabetical order; capitalize only proper names; and separate key words by semicolons)
graphite; high temperature; laser, mass spectrometry,; refractory materials; thermochemistry; vaporization.

13. AVAILABILITY

☒ Unlimited

☐ For Official Distribution. Do Not Release to NTIS

☐ Order From Superintendent of Documents, U.S. Government Printing Office, Washington, D.C. 20402.

☒ Order From National Technical Information Service (NTIS), Springfield, VA. 22161

14. NO. OF PRINTED PAGES

44

15. Price

$11.95